Maastricht University

Adding Speckle-Tracking Echocardiography to Visual Assessment of Systolic Wall Motion Abnormalities Improves the Detection of Myocardial Infarction

Please check the document version of this publication:

• A submitted manuscript is the version of the article upon submission and before peer-review. There can be important differences between the submitted version and the official published version of record. People interested in the research are advised to contact the author for the final version of the publication, or visit the DOI to the publisher's website.
• The final author version and the galley proof are versions of the publication after peer review.
• The final published version features the final layout of the paper including the volume, issue and page numbers.
Link to publication

Adding Speckle-Tracking Echocardiography to Visual Assessment of Systolic Wall Motion Abnormalities Improves the Detection of Myocardial Infarction

Manouk J. W. van Mourik, MD, Daniëlle V. J. Zaar, MD, Martijn W. Smulders, MD, Jordi Heijman, PhD, Joost Lumens, PhD, Jeffrey E. Dokter, MD, Valeria Lima Passos, PhD, Simon Schalla, MD, PhD, Christian Knackstedt, MD, PhD, Georg Schummers, MSc, Ola Gjesdal, MD, PhD, Thor Edvardsen, MD, PhD, and Sebastiaan C. A. M. Bekkers, MD, PhD, *Maastricht, the Netherlands; Bordeaux, France; Unterschleissheim, Germany; and Oslo, Norway*

Background: The aim of this study was to investigate whether speckle-tracking echocardiography (STE) improves the detection of myocardial infarction (MI) over visual assessment of systolic wall motion abnormalities (SWMAs) using delayed enhancement cardiac magnetic resonance imaging as a reference.

Methods: Transthoracic echocardiography was performed in 95 patients with first ST segment elevation MI 110 days (interquartile range, 97–171 days) after MI and in 48 healthy control subjects. Two experienced observers independently assessed SWMAs. Separately, longitudinal peak negative, peak systolic, end-systolic, global strain, and strain rate were measured and averaged for the American Heart Association–recommended coronary artery perfusion territories. Receiver operating characteristic analysis was used to determine a single optimal cutoff value for each strain parameter. The diagnostic accuracy of an algorithm combining visual assessment and STE was evaluated.

Results: Median infarct size and transmurality were 15% (interquartile range, 7%–24%) and 64% (interquartile range, 46%–78%), respectively. Sensitivity, specificity, and accuracy of visual assessment to detect MI were 74% (95% CI, 63%–82%), 85% (95% CI, 72%–93%), and 78% (95% CI, 70%–84%), respectively. Among the strain parameters, SR had the highest diagnostic accuracy (area under the curve, 0.88; 95% CI, 0.83–0.94; cutoff value, $-0.97 \ \text{sec}^{-1}$). The combination with STE improved sensitivity compared with visual assessment alone (94%; 95% CI, 86%–97%; $P < .001$), minimally affecting specificity (79%; 95% CI, 65%–89%; $P = .607$). Overall accuracy improved to 89% (95% CI, 82%–93%; $P = .011$). Multivariate analysis accounting for age and sex demonstrated that SR was independently associated with MI (odds ratio, 2.0; 95% CI, 1.6–2.7).

Conclusions: The sensitivity and diagnostic accuracy of visually detecting chronic MI by assessing SWMAs are moderate but substantially improve when adding STE. (J Am Soc Echocardiogr 2019;32:65-73.)

Keywords: Myocardial infarction, Transthoracic echocardiography, Deformation analysis, Strain, Speckle-tracking echocardiography, Cardiac magnetic resonance imaging

Abbreviations
CMR = Cardiac magnetic resonance imaging
DE = Delayed enhancement
IQR = Interquartile range
LV = Left ventricular
MI = Myocardial infarction
NPV = Negative predictive value
NRI = Net reclassification improvement
PPV = Positive predictive value
SR = Strain rate
STE = Speckle-tracking echocardiography
SWMA = Systolic wall motion abnormality
TTE = Transthoracic echocardiography

Community-based cohort and clinical studies have reported that a large proportion of myocardial infarctions (MIs) remain unrecognized because symptoms are either absent or atypical.[1,2] Unrecognized MIs tend to be smaller than recognized MIs and to occur more often in women, patients with diabetes, and the elderly. Remarkably, patients with subclinical MIs have higher mortality than patients without MI, and their mortality may even approach that of patients with clinically overt MIs.[1,3]

Delayed enhancement (DE) cardiac magnetic resonance imaging (CMR) is considered the reference technique for chronic ischemic myocardial injury and is sufficiently sensitive to detect small and subendocardial MI.[4,5] Nevertheless, DE CMR is not suitable for generalized screening. On the other hand, echocardiography is used in daily practice in both emergency and outpatient clinic settings to assess the presence and extent of regional systolic wall motion abnormalities (SWMAs) as a hallmark of MI.[6] However, the sensitivity of echocardiography for detecting MI varies widely depending on size, transmurality, and chronicity of MI.[7,8] Furthermore, visual assessment of SWMAs is subjective and highly operator and image quality dependent.[9,10]

Echocardiographic assessment of myocardial deformation using either tissue Doppler or speckle-tracking echocardiography (STE) allows a more objective estimation of regional contraction.[11,12] Despite suboptimal frame rates, STE is generally preferred over Doppler-based strain imaging because it measures deformation by tracking naturally occurring acoustic markers in the myocardium and is therefore less angle dependent.[13] Previous studies have shown high sensitivity and specificity of different strain parameters to differentiate among normal, subendocardial, and transmural MI, but the added value of STE to visual assessment to detect SWMAs is yet unknown.[10,14-20]

In this study, we investigated whether adding STE-based strain imaging to visual assessment by SWMAs improves the diagnostic accuracy to detect a chronic MI, using DE CMR as a reference standard.

METHODS

Consecutive patients were recruited from two observational studies that were originally designed to investigate infarct characteristics at baseline and follow-up using standard two-dimensional echocardiography and DE CMR in patients admitted with first ST segment elevation MI. The present study is a subanalysis of patients who underwent echocardiography and had evident scar on DE CMR at 3- to 6-month follow-up. Patients <18 years of age, those in atrial fibrillation at the time of examination, and those with typical contraindications to CMR were excluded. In total, 95 of 116 consecutive patients previously treated with primary percutaneous coronary intervention for first ST-segment elevation MI and 48 healthy control subjects were prospectively recruited from Maastricht University Medical Center+ in the Netherlands (60 patients and 33 control subjects) and Oslo University Hospital in Norway (35 patients and 15 control subjects). All patients received medical treatment according to guidelines at the time of the main studies.[21] Control subjects were either healthy volunteers or patients initially analyzed for various reasons and finally diagnosed without cardiac disease (normal left ventricular [LV] function, absence of myocardial scar on DE CMR, and absence of significant coronary artery disease after invasive or noninvasive testing). To represent daily clinical practice, patients were not excluded because of poor echocardiographic image quality. The investigation conformed to the principles outlined in the Declaration of Helsinki, and both centers conformed to local ethical regulations (MEC 05-199 and S-03115). Informed consent was obtained from all patients.

Transthoracic Echocardiography

In patients, TTE was performed ≥3 months after admission (median, 110 days; interquartile range [IQR], 97–171 days). All images were acquired in the left lateral decubitus position and recorded as electrocardiographically gated digital loops and stored for offline analysis. Standard TTE was performed according to the American Society of Echocardiography guidelines using commercially available ultrasound systems with phased-array transducers (Sonos 5500 or iE33 [Philips Medical Systems, Best, the Netherlands] or Vivid 5 or 7 [GE Vingmed Ultrasound, Horten, Norway]). Because the objectives of the two main studies did not include investigating STE, image acquisition was not specifically optimized for this purpose, resulting in suboptimal frame rates (48 ± 9 Hz). All echocardiographic images were placed in random order and independently analyzed by two experienced cardiologists who were blinded to the clinical, speckle-tracking echocardiographic, and DE CMR data. Visual assessment of SWMAs was performed on all available images (apical and parasternal views), whereas STE was analyzed in the apical two-, three-, and four-chamber views only.

Visual Assessment

Regional SWMAs were assessed as previously described but modified to the American Heart Association 17-segment model and scored as normal, hypokinetic, akinetic, or dyskinetic.[22] For segments depicted in multiple views, a final conclusion was made by combining all views. Each observer finally concluded whether SWMAs were definitely or possibly present or definitely absent. Discrepancies were resolved in consensus with a third experienced observer for a final conclusion. A patient was classified as having MI when at least one segment was abnormal. To determine the accuracy of the visual assessment, possible and definite SWMAs were combined and considered as indicating the presence of MI. Image quality was scored as poor (if at least one segment was not interpretable in any view), average (all segments were interpretable but not in all views), or excellent (all segments were interpretable in all views).

Speckle-Tracking Echocardiography

Longitudinal strain and strain rate (SR) were measured offline in the apical two-, three-, and four-chamber images using dedicated vendor-independent software (2D CPA; TomTec Imaging Systems, Unterschleissheim, Germany). The regions of interest were manually

outlined by marking the endocardial and epicardial borders in the end-systolic frame. End-systole was defined as aortic valve closure, the end of the electrocardiographic T wave, or before mitral valve opening. The software automatically tracks myocardial speckle patterns frame by frame during one cardiac cycle (R-R interval) and generates LV strain parameters for each of the 17 segments. Suboptimal tracking was manually corrected. Segmental tracking quality was scored by an observer on a three-point scale (0 = poor tracking despite multiple attempts to optimize contours, 1 = minimal adjustment necessary, and 2 = no adjustment necessary). A global tracking quality score (ranging between 0 and 34) was calculated by summing each segmental tracking quality score. For this study, multiple segmental longitudinal strain parameters were acquired: peak negative strain, end-systolic strain, peak systolic strain (defined as either peak positive or negative strain during systole), and peak systolic negative SR.[23] For segments depicted in multiple views (segments 14, 16, and 17), an average value was calculated. Territorial strain was calculated on the basis of the perfusion territories of the three major coronary arteries in the 17-segment LV model, by averaging all segmental strain values within each territory (segments 1, 2, 7, 8, 13, 14, and 17 for the left anterior descending coronary artery; segments 5, 6, 11, 12, and 16 for the circumflex coronary artery; and segments 3, 4, 9, 10, and 15 for the right coronary artery). Peak negative strain values from all 17 segments were averaged to assess LV global longitudinal strain.

Cardiovascular Magnetic Resonance

CMR was performed 111 days (IQR, 99–173 days) after admission and shortly after TTE (1 day; IQR, 0–3 days). Images were acquired with 1.5-T systems (Intera [Philips Medical Systems] and Magnetom Vision Plus or Magnetom Sonata [Siemens Medical Systems, Erlangen, Germany]) equipped with dedicated cardiac software and phased-array surface coils. Cine images were acquired in multiple short-axis views covering the left ventricle and three long-axis views using steady-state free precession sequences. DE CMR images were acquired in multiple short-axis slices covering the left ventricle 10 to 15 min after the administration of a gadolinium-based contrast agent, using a breath-hold segmented inversion recovery sequence. Inversion delay time was set to null signal from normal myocardium. CMR images were analyzed by a level 3–accredited cardiologist blinded to clinical and echocardiographic data, using dedicated software (CAAS MRV 4.2; Pie Medical Imaging, Maastricht, the Netherlands). LV volumes, mass, and ejection fraction were measured using manual planimetry of endocardial and epicardial borders at end-diastole and end-systole in the stack of short-axis cine images. Infarct size and transmurality were measured on the short-axis DE magnitude images as hyperenhanced regions using the full-width half-maximum method.[24] Transmural extent of infarction was calculated by dividing the hyperenhanced area by the total area of the predefined segment. Subendocardial MI was defined as <50% transmurality. Total infarct size was expressed as a percentage of LV myocardial mass.

Observer Variability

Several months later, the same two observers repeated the visual assessment and speckle-tracking echocardiographic analysis in 10 randomly selected subjects, blinded to the results of the first analysis and to clinical and CMR data. Cohen's κ coefficient and the intraclass correlation coefficient were used to determine both inter- and intra-observer variability.

Statistical Analysis

Continuous variables with normal distribution are expressed as mean ± SD and otherwise as median with IQR. Continuous variables were compared using independent Student's t tests or the Mann-Whitney U test, as appropriate. Differences in categorical variables were evaluated using the χ^2 or Fisher exact test. For each individual strain parameter, receiver operating characteristic curves were computed to determine the area under the curve and to determine a single optimal cutoff value to detect MI on the basis of the maximum sum of sensitivity and specificity (Youden's index). MI classification was considered correct if abnormal strain values were found in the appropriate and matching infarcted quadrants. Abnormal strain in neighboring or opposing quadrants solely was considered a false-negative finding. Sensitivity, specificity, positive predictive value (PPV), negative predictive value (NPV), and overall diagnostic accuracy including their related 95% CIs to detect MI were calculated for the visual assessment of SWMAs, each strain parameter separately, and for an algorithm that combined visual assessment of SWMAs with the best strain parameter. Differences in sensitivity, specificity, and diagnostic accuracy between visual assessment and the algorithm were tested using the McNemar test.[25] Categorical net reclassification improvement (NRI) was used to test the performance of the algorithm in comparison with visual assessment only (+1, 0, or −1 was scored for patients who were correctly, not, or wrongly reclassified). Finally, a multivariate logistic regression model was fitted to demonstrate the added value of STE to detect MI, after adjusting for baseline risk factors (age and sex). SPSS version 21.0 (SPSS, Chicago, IL) was used for all statistical analyses. A two-tailed P value < .05 was considered to indicate statistical significance.

RESULTS

Baseline Characteristics

Patients were more often male (80% vs 54%, P = .001) and older compared with healthy control subjects (59 ± 11 vs 47 ± 12 years, P < .001; Table 1). The culprit coronary artery was the left anterior descending coronary artery in approximately half of patients (49%), and more than half had single-vessel disease (57%). Median infarct transmurality and total LV infarct size were 64% (IQR, 46%–78%) and 15% of LV mass (IQR, 7%–24%), respectively. LV ejection fraction assessed by CMR was significantly lower in patients compared with healthy control subjects (54 ± 10% vs 61 ± 5%, P < .001).

For the visual assessment of SWMAs, overall echocardiographic image quality was graded as average (36%) or excellent (58%)

Table 1 Baseline characteristics

Characteristic	Patients (*N* = 95)	Control subjects (*n* = 48)	*P*
Patient characteristics			
Age (y)	59 ± 11	47 ± 12	<.001
Men	76 (80)	26 (54)	.001
Angiographic characteristics			
Infarct-related artery			
LAD	47 (49)		
RCA	37 (39)		
RCx	11 (12)		
Number of diseased vessels			
Single	54 (57)		
Multiple	41 (43)		
TIMI grade 3 flow			
Pre-PCI	11 (12)		
Post-PCI	90 (95)		
Location			
Anterior MI	47 (49)		
Nonanterior MI	48 (51)		
Echocardiographic characteristics			
Days after MI	110 (97–171)		
Image quality			.485
Excellent	36 (38)	15 (31)	
Average	52 (55)	31 (65)	
Poor	7 (7)	2 (4)	
STE tracking quality	14 ± 5	14 ± 5	.473
GLS (%)	−12.3 ± 3.0	−15.7 ± 2.3	<.001
CMR characteristics			
Days after MI	111 (99–173)		
Days between echocardiography and CMR	0 (0–3)		
Infarct size (% of left ventricle)	15 (7–24)		
Infarct transmurality (%)	64 (46–78)		
Ejection fraction (%)	54 ± 10	61 ± 5	<.001

GLS, Global longitudinal strain; *LAD*, left anterior descending coronary artery; *PCI*, percutaneous coronary intervention; *RCA*, right coronary artery; *RCx*, right circumflex artery; *TIMI*, Thrombolysis in Myocardial Infarction.
Data are expressed as mean ± SD, number (percentage), or median (IQR).

and as poor in only 6%. Image quality did not differ between patients and control subjects (*P* = .485). Overall tracking quality score was 14 ± 5 and was similar between patients and control subjects (*P* = .473).

Visual Assessment

Visual assessment of SWMAs correctly identified 70 of 95 patients with MI when possible and definite MI were combined to indicate the presence of MI, resulting in a 74% sensitivity (95% CI, 63%–82%; Tables 2 and 3). In the control group, seven subjects were incorrectly classified as having MI, resulting in 85% specificity

Table 2 Visual assessment of identifying MI

MI present	Control subjects	Patients with MI*	Total
Definitely no	41	25	66
Possibly yes[†]	7	15	22
Definitely yes[†]	0	55	55
Total	48	95	143

*MI as detected by DE-CMR.
[†]Possibly and definitely combined to calculate sensitivity and specificity (see text).

Table 3 Diagnostic accuracy of visual assessment, SR, and the combined algorithm to identify MI

Diagnostic value	Visual assessment, % (95% CI)	SR, % (95% CI)	Algorithm, % (95% CI)	P
Sensitivity	74 (63–82)*	85 (76–91)	94 (86–97)*	<.001
Specificity	85 (72–93)*	79 (65–89)	79 (65–89)*	.607
NPV	62 (49–74)	73 (59–84)	86 (72–94)	
PPV	91 (82–96)	89 (80–94)	90 (82–95)	
Accuracy	78 (70–84)*	83 (76–89)	89 (82–93)*	.011

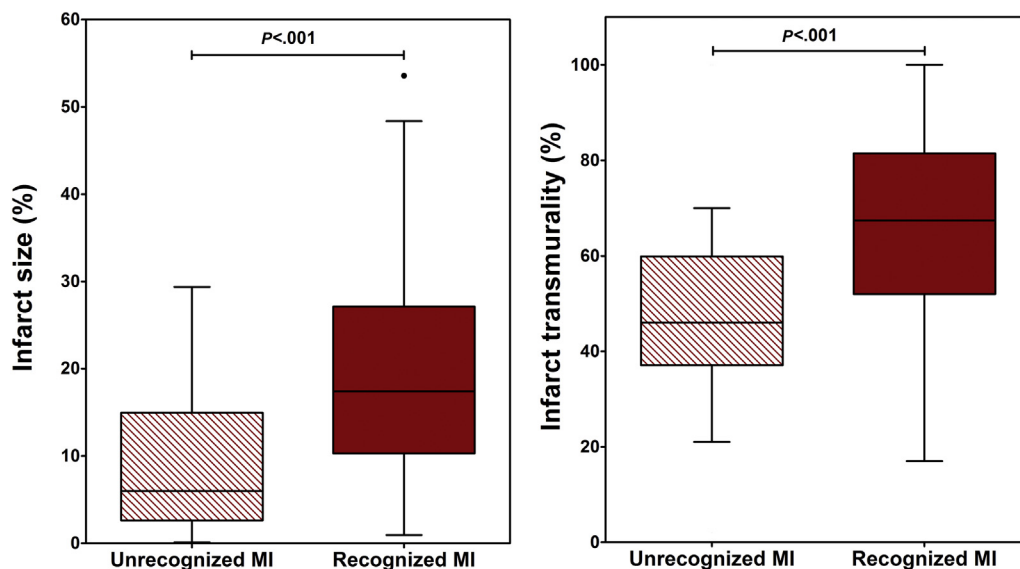*P value between visual assessment and the algorithm.

Figure 1 Identification of MI by visual assessment in relation to infarct size (*left*) and transmurality (*right*).

(95% CI, 72%–93%). The NPV was 62% (95% CI, 49%–74%). The PPV was 91% (95% CI, 82%–96%) but was 100% (95% CI, 92%–100%) when only definite SWMAs were taken into account. Compared with correctly identified MIs, those that were not detected by visual assessment (n = 25) were smaller (6% [IQR, 3%–15%] vs 17% [IQR, 10%–27%], P < .001), less transmural (46% [IQR, 37%–60%] vs 67% [IQR, 52%–81%], P < .001; Figure 1) and more often located nonanterior (76% vs 41%, P = .003).

Speckle-Tracking Echocardiography

The results of receiver operating characteristic analysis of each strain parameter to identify MI are shown in Figure 2. Of all strain parameters tested, SR had the largest area under the curve (0.88; 95% CI, 0.83-0.94). With respect to overall accuracy, SR performed significantly better than end-systolic strain as the second best parameter (83% [95% CI, 76%–89%] vs 71% [95% CI, 62%–77%], respectively, P = .006). The optimal cutoff value for SR was set at −0.97 sec^{-1}. Using this value, 88 of 95 patients were correctly identified, resulting in sensitivity of 85% (95% CI, 76%–89%). Of 48 control subjects, 38 were correctly classified without MI, resulting in specificity of 79% (95% CI, 65%–89%). The NPV and PPV were 73% (95% CI, 59%–84%) and 89% (95% CI, 80%–94%), respectively (Table 3).

Observer Variability

Analysis of intraobserver variability of the visual assessment showed agreement of 80% ($\kappa = 0.58$) and 85% ($\kappa = 0.70$) for interobserver variability. The intraclass correlation coefficients for speckle-tracking echocardiographic analysis were 0.82 (95% CI, 0.68–0.90) and 0.89 (95% CI, 0.80–0.94), respectively.

Algorithm Combining Visual Assessment and STE

Subsequently, the diagnostic accuracy of an algorithm that combined visual assessment and STE (SR) was investigated. STE was not performed when SWMAs were definitely present, because in this subgroup the PPV was already 100%. Accordingly, STE was performed in only 88 cases graded as having possible or no MI. Here, abnormal SR (i.e., ≥−0.97 sec^{-1}) identified 34 additional patients with MI, while only six remained undetected. This resulted in a significant increase in sensitivity compared with visual assessment only (94% [95% CI, 86%–97%] vs 74% [95% CI, 63%–82%], P < .001; Table 3, Figure 3), with minimal effect on specificity (79% [95% CI, 65%–89%] vs 85% [95% CI, 72%–93%], P = .607). Overall, diagnostic accuracy of the algorithm was significantly higher than visual assessment only (89% [95% CI, 82%–93%] vs 78% [95% CI, 70%–84%], respectively, P = .011). This improvement was confirmed
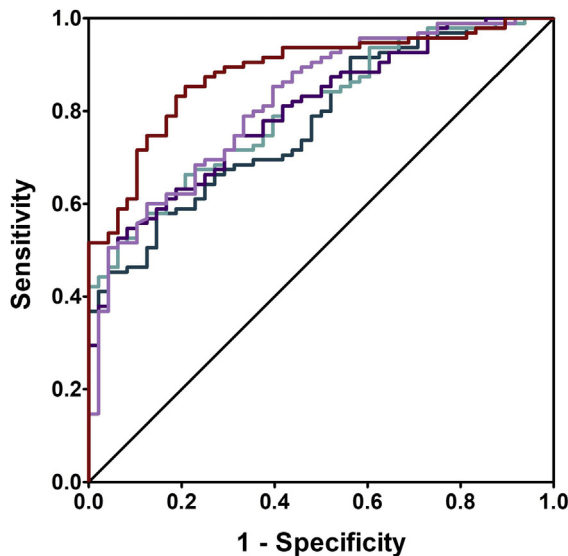
		AUC (%, 95%CI)	Optimal cut-off	Accuracy (%, 95%CI)
	SR	0.88 (0.83-0.94)	-0.97 s⁻¹	83 (76-91) *
	GLS	0.82 (0.75-0.89)	-13.6%	69 (61-77)
	PSS	0.80 (0.73-0.87)	-10.9%	67 (59-75)
	ESS	0.80 (0.73-0.87)	-10.6%	71 (62-77) *
	PNS	0.77 (0.70-0.85)	-12.7%	67 (59-75)

Figure 2 Receiver operating characteristic curves of individual strain parameters to identify MI (*top*); area under the curve (AUC) values, optimal cutoff values, and accuracies (*bottom*). *P* = .006. *ESS*, End-systolic strain; *GLS*, global longitudinal strain; *PNS*, peak negative strain; *PSS*, peak systolic strain.

by reclassification analysis. Using the algorithm, a large proportion of patients with MI could be correctly reclassified (NRI = 0.2000), while only a few healthy control subjects were incorrectly reclassified as having MI (NRI = −0.0625). A total NRI of 0.1375 indicates that the algorithm resulted in improved overall classification.

Subgroup and Multivariate Analysis

The additional value of SR over visual assessment was especially evident in less transmural and smaller MI. The sensitivity of visual assessment and SR to detect ≥50% transmural and larger MI (≥15% of LV mass) was similar (86% [95% CI, 75%–93%] vs 86% [95% CI, 75%–93%], *P* = 1.000, and 87% [95% CI, 74%–95%] vs 85% [95% CI, 71%–93%], *P* = 1.000, respectively). In contrast, the sensitivity of visually detecting <50% transmural and smaller MI (<15% of LV mass) was low but substantially improved when using SR (47% [95% CI, 29%–65%] vs 83% [95% CI, 65%–94%], *P* = .013, and 60% [95% CI, 45%–74%] vs 85% [95% CI, 71%–93%], *P* = .012, respectively). Patient examples are shown in Figure 4. Representative supplemental echocardiographic cine loops are available online (Videos 1 and 2 available at www.onlinejase.com). Age and male gender were significantly associated with MI, with, respectively, mutually adjusted odds ratios of 1.1 (95% CI, 1.1-1.1) and 3.8 (95% CI, 1.6-9.1). Noticeably, SR remained independently associated with the

same outcome after adjustment for these variables (odds ratio, 2.0; 95% CI, 1.6–2.7; Table 4).

DISCUSSION

The present study demonstrates that the overall diagnostic accuracy of identifying a 3-month-old MI by assessing regional SWMAs is only moderate and can be significantly improved by adding strain imaging using STE. Our combined algorithm increased the proportion of accurately detected MI by 27%. The improved sensitivity came at the cost of only a modest, nonsignificant decrease (6%) in specificity. Of all strain imaging indices investigated, SR was most accurate.

An MI may be asymptomatic or associated with atypical symptoms and therefore remain unrecognized by patients and health care professionals when Q waves are absent. Unrecognized MIs are prevalent, ranging from 17% in community-based studies to 25% to 27% in patients with known or suspected coronary artery disease.[1,26] Because patients with unrecognized MI have a similar long-term prognosis as those with clinically recognized MI, it is important that they be accurately detected enabling adequate therapeutic strategies.[1]

By means of detecting reduced regional wall thickening as a hallmark of MI, echocardiography has generally been regarded an accurate tool to evaluate regional LV function. However, visual analysis of SWMAs is less sensitive to detect chronic than acute MI because the contractility of initially stunned myocardium may improve over time after successful reperfusion.[27] Furthermore, the appearance and persistence of SWMAs are strongly dependent on infarct size and transmurality.[8] Improved reperfusion strategies over time have further limited infarct size, making accurate detection of MI using SWMAs even more challenging in the present era. Finally, visual analysis of wall motion abnormalities suffers from relatively low interobserver agreement.[9] Our results confirm the overall moderate sensitivity (74%; 95% CI, 63%–82%) to detect a chronic MI by visual assessment and its relation to infarct size and transmurality. On the other hand, the PPV to detect MI by visual analysis of SWMAs was high (91%; 95% CI, 82%–96%). Indeed, all subjects with definite SWMAs were correctly identified as having MI, indicating that larger MIs are easily identified by experienced cardiologists.

Myocardial velocity or deformation imaging using Doppler tissue imaging or STE allows a more objective quantification of global and regional myocardial function and identification of more subtle changes in systolic function than visual assessment.[13,28] Strain imaging has been shown to be useful in ischemic as well as various nonischemic myocardial diseases.[13,29] Up to now, the majority of studies using strain imaging in ischemic heart disease have investigated its relation with quantitative measures of infarct size and transmurality using DE CMR as a reference standard.[10,14,18] In patients with chronic MI, Gjesdal *et al.*[30] demonstrated that global longitudinal and circumferential strain by STE are able to differentiate between small (<30 g), medium (30–50 g), and large MI (>50 g), whereas assessment of SWMAs was not. Others have shown that assessment of regional SWMAs and global longitudinal strain are accurate and independent predictors of infarct size ≥12% and that combined use did not improve diagnostic accuracy.[31] A study involving different vendors recently showed that segmental longitudinal strain

Visual assessment of SWMA
(n=143)

Definite SWMA (n=55)   **Possible SWMA** (n=22)   **No SWMA** (n=66)

Additional SR (n=88)

SR abnormal (n=44)   **SR normal** (n=44)

MI* (n=55)   **Control** (n=0)   **MI*** (n=34)   **Control** (n=10)   **MI*** (n=6)   **Control** (n=38)
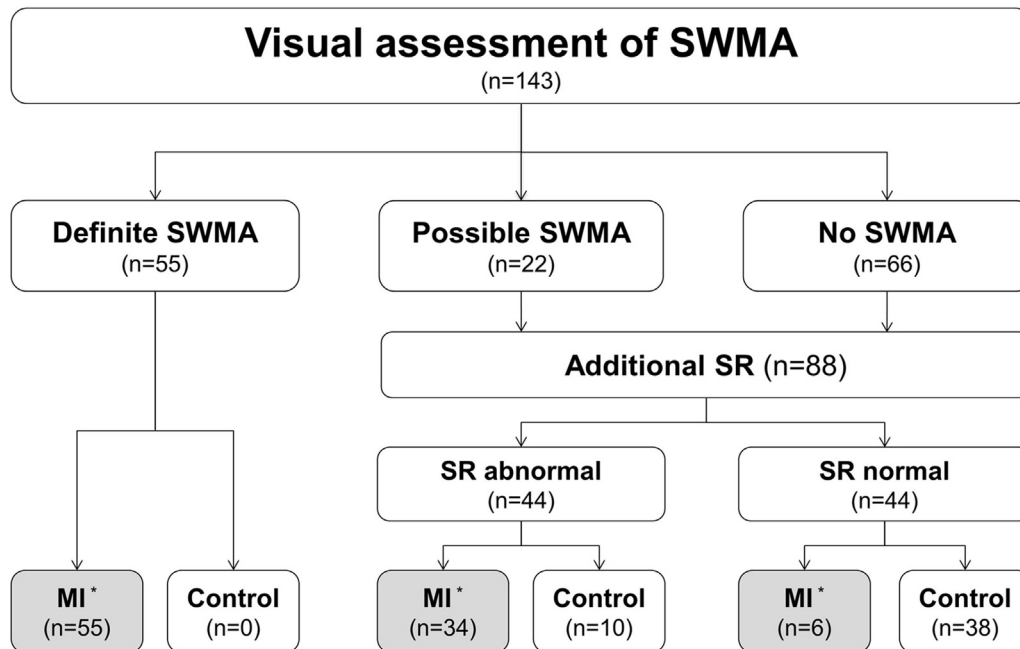
Figure 3 Algorithm combining visual assessment and SR to identify MI. *MI as detected by DE CMR.

accurately discriminated between transmural and noninfarcted segments.[32] It is well known that longitudinal LV strain is lower in men than women and decreases with increasing age.[33] However, after adjusting for both variables SR remained independently associated with MI detection in the present study.

Our study is one of few studies investigating whether strain imaging can be used to identify MI more accurately. Using gated stress ^{99m}Tc sestamibi single-photon emission computed tomography as a reference standard, Mele et al.[34] showed that SR is more sensitive and specific than visual wall motion analysis to detect infarcted segments (91% vs. 78% and 84% vs. 71%, respectively).[34] On the other hand, Støylen et al.[35] found that SR analysis using color Doppler tissue imaging had similar sensitivity and specificity as visual wall motion scoring to detect MI. Combining visual scoring and SR imaging did not change classification accuracy in their study. This may be explained by less accurate detection of MI using semiquantitative measures on the basis of color-coded SR imaging maps than using quantitative cutoff values.

Myocardial ischemia first affects the subendocardial layers that predominantly contain longitudinal myocardial fibers resulting in reduced longitudinal shortening.[36] Circumferential and radial function start to decrease only when infarct transmurality exceeds 50%, allowing visual detection of reduced radial thickening. This is in accordance with our subgroup analysis demonstrating lower sensitivity of visual detection of smaller and subendocardial infarcts. In addition to being subjective, visual wall motion scoring is a crude, discontinuous way of infarct analysis. Deformation analysis uses a continuous scale, allowing better differentiation between levels of dysfunction and identification of smaller MI. Of all strain indices investigated (i.e., peak negative strain, end-systolic strain, peak systolic strain, global longitudinal strain, and SR), SR appeared most accurate to detect MI. Although speculative, this may indicate that SR, being the rate of systolic shortening, is affected by both diminished contraction due to loss of myocytes and slowing of conduction in the infarcted area.

LIMITATIONS

Given the considerable intervendor measurement variability of myocardial deformation and the related lack of reference strain values, the use of absolute cutoff values for strain-based clinical decision making is currently not recommended. It was not our goal to define specific cutoff values for strain or SR indices that can be universally applied for MI detection but rather to demonstrate the added value of strain imaging to routine echocardiographic evaluation. Furthermore, future studies are needed to evaluate how specific a decrease of systolic SR is for ischemic heart disease or MI, in particular in patients with conduction abnormalities.

The PPV, NPV, and accuracy of a test are related to the prevalence of disease, which was much higher in this study (66%) than generally encountered in the real-world echocardiography laboratory, potentially increasing the number of false positives when using STE. At the same time, the sensitivity of visually detecting MI in the echocardiography laboratory will be even lower than observed in this study because of this lower prevalence of disease. Furthermore, we believe that high sensitivity of a test (i.e., SR) justifies lower specificity and the associated risk for overdiagnosis when dealing with "life-threatening" diseases such as MI. Our algorithm needs further validation for use in daily practice, for example, in a cohort encompassing various myocardial pathologies or, ideally but less practical, evaluation in daily practice using DE CMR as a reference standard.

Although image acquisition was not specifically optimized for speckle-tracking echocardiographic analysis, resulting in suboptimal frame rates (48 ± 9 Hz), our results suggest that performance may still be reliable even at lower than recommended frame-rates for STE (50–90 Hz).

CONCLUSION

We have demonstrated that adding strain and SR imaging to visual assessment of SWMAs significantly improved the diagnostic accuracy
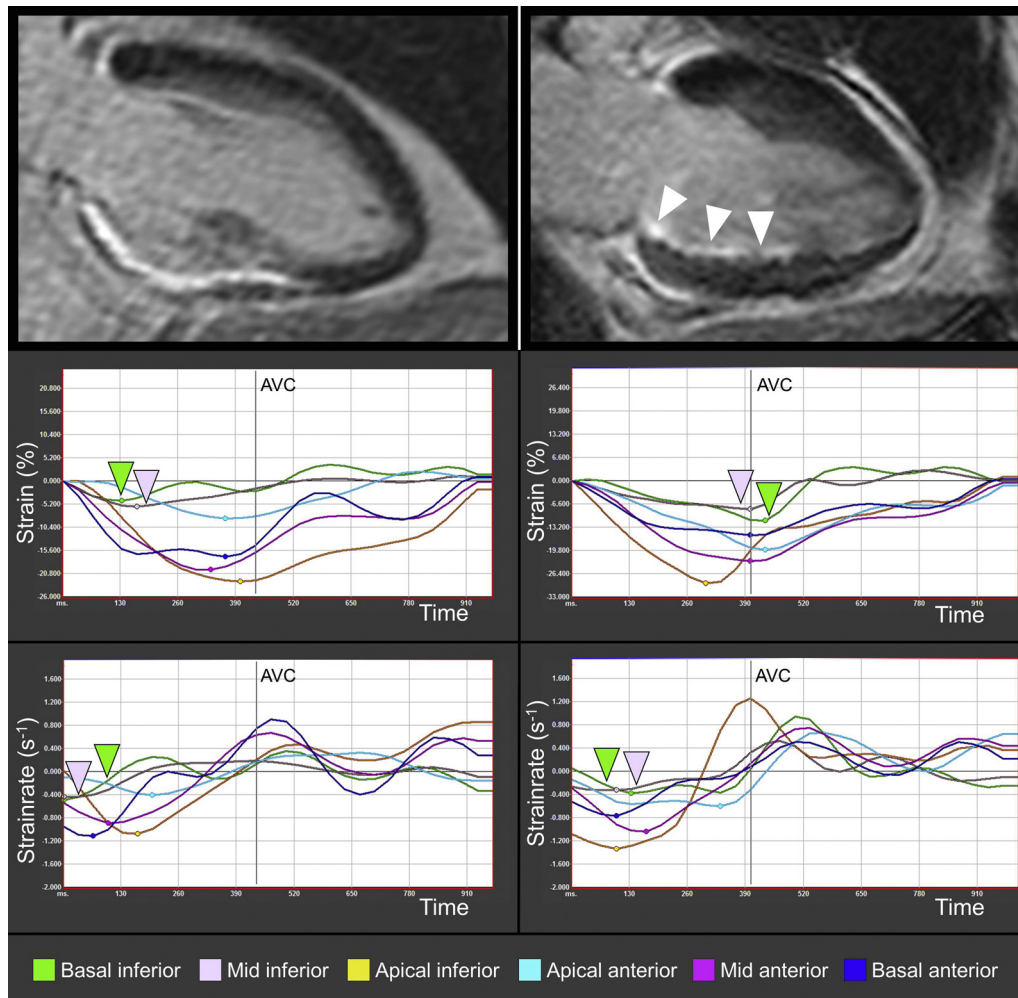
Figure 4 Patient examples with different levels of infarct transmurality. DE CMR images showing a transmural MI (85%) of the basal-mid inferior segments (*top left*) with abnormal strain and SR (*middle and lower left*) and a subendocardial (14%) MI of the basal-mid inferior segments (*white arrowheads*; *top right*) without convincing regional SWMAs but with abnormal strain and SR (*middle and lower right*). Supplemental corresponding echocardiographic cine loops (Videos 1 and 2) are available online. *AVC*, Aortic valve closure.

Table 4 Multivariate binary logistic regression analysis

	Model 1		Model 2	
Characteristic	Or (95% CI)	P	Or (95% CI)	P
Age	1.1 (1.1–1.1)	<.001	1.1 (1.0–1.1)	<.001
Gender	3.8 (1.6–9.1)	.003	2.8 (1.0–8.0)	.054
SR			2.0 (1.6–2.7)*	<.001
AUC	0.82 (0.75–0.89)†		0.92 (0.88–0.97)†	.009†

AUC, Area under the curve; *OR*, odds ratio.
*For each 0.1 $\sec^{-1}$ increment.
†Adding SR to the prediction model significantly improves the AUC.

to detect chronic MI. The sensitivity and overall diagnostic accuracy to identify chronic MI by visually assessing regional wall motion alone were only moderate, and our results therefore imply that strain and SR imaging appears to be a valuable addition to routine echocardiography.

SUPPLEMENTARY DATA

Supplementary data to this article can be found online at https://doi.org/10.1016/j.echo.2018.09.007.

REFERENCES

1. Schelbert EB, Cao JJ, Sigurdsson S, Aspelund T, Kellman P, Aletras AH, et al. Prevalence and prognosis of unrecognized myocardial infarction determined by cardiac magnetic resonance in older adults. JAMA 2012; 308:890-6.
2. Turkbey EB, Nacif MS, Guo M, McClelland RL, Teixeira PB, Bild DE, et al. Prevalence and correlates of myocardial scar in a US cohort. JAMA 2015; 314:1945-54.
3. Barbier CE, Themudo R, Bjerner T, Johansson L, Lind L, Ahlstrom H. Long-term prognosis of unrecognized myocardial infarction detected with cardiovascular magnetic resonance in an elderly population. J Cardiovasc Magn Reson 2016;18:43.
4. Kim RJ, Fieno DS, Parrish TB, Harris K, Chen EL, Simonetti O, et al. Relationship of MRI delayed contrast enhancement to irreversible

injury, infarct age, and contractile function. Circulation 1999;100:1992-2002.

5. Wagner A, Mahrholdt H, Holly TA, Elliott MD, Regenfus M, Parker M, et al. Contrast-enhanced MRI and routine single photon emission computed tomography (SPECT) perfusion imaging for detection of subendocardial myocardial infarcts: an imaging study. Lancet 2003;361:374-9.

6. Prastaro M, Pirozzi E, Gaibazzi N, Paolillo S, Santoro C, Savarese G, et al. Expert review on the prognostic role of echocardiography after acute myocardial infarction. J Am Soc Echocardiogr 2017;30:431-43.e2.

7. Kontos MC. Role of echocardiography in the emergency department for identifying patients with myocardial infarction and ischemia. Echocardiography 1999;16:193-205.

8. Lieberman AN, Weiss JL, Jugdutt BI, Becker LC, Bulkley BH, Garrison JG, et al. Two-dimensional echocardiography and infarct size: relationship of regional wall motion and thickening to the extent of myocardial infarction in the dog. Circulation 1981;63:739-46.

9. Hoffmann R, Lethen H, Marwick T, Arnese M, Fioretti P, Pingitore A, et al. Analysis of interinstitutional observer agreement in interpretation of dobutamine stress echocardiograms. J Am Coll Cardiol 1996;27:330-6.

10. Zhang Y, Chan AK, Yu CM, Yip GW, Fung JW, Lam WW, et al. Strain rate imaging differentiates transmural from non-transmural myocardial infarction: a validation study using delayed-enhancement magnetic resonance imaging. J Am Coll Cardiol 2005;46:864-71.

11. D'Hooge J, Konofagou E, Jamal F, Heimdal A, Barrios L, Bijnens B, et al. Two-dimensional ultrasonic strain rate measurement of the human heart in vivo. IEEE Trans Ultrason Ferroelectr Freq Control 2002;49:281-6.

12. Urheim S, Edvardsen T, Torp H, Angelsen B, Smiseth OA. Myocardial strain by Doppler echocardiography. Validation of a new method to quantify regional myocardial function. Circulation 2000;102:1158-64.

13. Collier P, Phelan D, Klein A. A test in context: myocardial strain measured by speckle-tracking echocardiography. J Am Coll Cardiol 2017;69:1043-56.

14. Becker M, Hoffmann R, Kuhl HP, Grawe H, Katoh M, Kramann R, et al. Analysis of myocardial deformation based on ultrasonic pixel tracking to determine transmurality in chronic myocardial infarction. Eur Heart J 2006;27:2560-6.

15. Edvardsen T, Gerber BL, Garot J, Bluemke DA, Lima JA, Smiseth OA. Quantitative assessment of intrinsic regional myocardial deformation by Doppler strain rate echocardiography in humans: validation against three-dimensional tagged magnetic resonance imaging. Circulation 2002;106:50-6.

16. Gjesdal O, Helle-Valle T, Hopp E, Lunde K, Vartdal T, Aakhus S, et al. Noninvasive separation of large, medium, and small myocardial infarcts in survivors of reperfused ST-elevation myocardial infarction: a comprehensive tissue Doppler and speckle-tracking echocardiography study. Circ Cardiovasc Imaging 2008;1:189-96.

17. Jamal F, Kukulski T, Sutherland GR, Weidemann F, D'Hooge J, Bijnens B, et al. Can changes in systolic longitudinal deformation quantify regional myocardial function after an acute infarction? An ultrasonic strain rate and strain study. J Am Soc Echocardiogr 2002;15:723-30.

18. Sachdev V, Aletras AH, Padmanabhan S, Sidenko S, Rao YN, Brenneman CL, et al. Myocardial strain decreases with increasing transmurality of infarction: a Doppler echocardiographic and magnetic resonance correlation study. J Am Soc Echocardiogr 2006;19:34-9.

19. Voigt JU, Arnold MF, Karlsson M, Hubbert L, Kukulski T, Hatle L, et al. Assessment of regional longitudinal myocardial strain rate derived from Doppler myocardial imaging indexes in normal and infarcted myocardium. J Am Soc Echocardiogr 2000;13:588-98.

20. Altiok E, Tiemann S, Becker M, Koos R, Zwicker C, Schroeder J, et al. Myocardial deformation imaging by two-dimensional speckle-tracking echocardiography for prediction of global and segmental functional changes after acute myocardial infarction: a comparison with late gadolinium enhancement cardiac magnetic resonance. J Am Soc Echocardiogr 2014;27:249-57.

21. Van de Werf F, Ardissino D, Betriu A, Cokkinos DV, Falk E, Fox KA, et al. Management of acute myocardial infarction in patients presenting with ST-segment elevation. The Task Force on the Management of acute myocardial infarction of the European Society of Cardiology. Eur Heart J 2003;24:28-66.

22. Lang RM, Badano LP, Mor-Avi V, Afilalo J, Armstrong A, Ernande L, et al. Recommendations for cardiac chamber quantification by echocardiography in adults: an update from the American Society of echocardiography and the European association of cardiovascular imaging. J Am Soc Echocardiogr 2015;28:1-39.

23. Voigt JU, Pedrizzetti G, Lysyansky P, Marwick TH, Houle H, Baumann R, et al. Definitions for a common standard for 2D speckle tracking echocardiography: consensus document of the EACVI/ASE/Industry Task Force to standardize deformation imaging. J Am Soc Echocardiogr 2015;28:183-93.

24. Amado LC, Gerber BL, Gupta SN, Rettmann DW, Szarf G, Schock R, et al. Accurate and objective infarct sizing by contrast-enhanced magnetic resonance imaging in a canine myocardial infarction model. J Am Coll Cardiol 2004;44:2383-9.

25. Trajman A, Luiz RR. McNemar chi^2 test revisited: comparing sensitivity and specificity of diagnostic examinations. Scand J Clin Lab Invest 2008;68:77-80.

26. Kim HW, Klem I, Shah DJ, Wu E, Meyers SN, Parker MA, et al. Unrecognized non-Q-wave myocardial infarction: prevalence and prognostic significance in patients with suspected coronary disease. PLoS Med 2009;6:e1000057.

27. Bolli R. Mechanism of myocardial "stunning". Circulation 1990;82:723-38.

28. Edvardsen T, Skulstad H, Aakhus S, Urheim S, Ihlen H. Regional myocardial systolic function during acute myocardial ischemia assessed by strain Doppler echocardiography. J Am Coll Cardiol 2001;37:726-30.

29. Gorcsan J III, Tanaka H. Echocardiographic assessment of myocardial strain. J Am Coll Cardiol 2011;58:1401-13.

30. Gjesdal O, Hopp E, Vartdal T, Lunde K, Helle-Valle T, Aakhus S, et al. Global longitudinal strain measured by two-dimensional speckle tracking echocardiography is closely related to myocardial infarct size in chronic ischaemic heart disease. Clin Sci (Lond) 2007;113:287-96.

31. Eek C, Grenne B, Brunvand H, Aakhus S, Endresen K, Hol PK, et al. Strain echocardiography and wall motion score index predicts final infarct size in patients with non-ST-segment-elevation myocardial infarction. Circ Cardiovasc Imaging 2010;3:187-94.

32. Mirea O, Pagourelias ED, Duchenne J, Bogaert J, Thomas JD, Badano LP, et al. Intervendor differences in the accuracy of detecting regional functional abnormalities: a report from the EACVI-ASE Strain Standardization Task Force. JACC Cardiovasc Imaging 2018;11:25-34.

33. Sugimoto T, Dulgheru R, Bernard A, Ilardi F, Contu L, Addetia K, et al. Echocardiographic reference ranges for normal left ventricular 2D strain: results from the EACVI NORRE study. Eur Heart J Cardiovasc Imaging 2017;18:833-40.

34. Mele D, Pasanisi G, Heimdal A, Cittanti C, Guardigli G, Levine RA, et al. Improved recognition of dysfunctioning myocardial segments by longitudinal strain rate versus velocity in patients with myocardial infarction. J Am Soc Echocardiogr 2004;17:313-21.

35. Støylen A, Heimdal A, Bjornstad K, Wiseth R, Vik-Mo H, Torp H, et al. Strain rate imaging by ultrasonography in the diagnosis of coronary artery disease. J Am Soc Echocardiogr 2000;13:1053-64.

36. Chan J, Hanekom L, Wong C, Leano R, Cho GY, Marwick TH. Differentiation of subendocardial and transmural infarction using two-dimensional strain rate imaging to assess short-axis and long-axis myocardial function. J Am Coll Cardiol 2006;48:2026-33.